Journal of Neuroscience Methods 120 (2002) 131–143

JOURNAL OF NEUROSCIENCE METHODS

www.elsevier.com/locate/jneumeth

Parameter-extraction of a two-compartment model for whole-cell data analysis

Santosh Pandey *, Marvin H. White

Sherman Fairchild Center, Lehigh University, Bethlehem, PA 18015, USA

Received 10 April 2002; received in revised form 2 July 2002; accepted 3 July 2002

Abstract

Neuronal modeling of patch-clamp data is based on approximations which are valid under specific assumptions regarding cell properties and morphology. Certain cells, which show a biexponential capacitance transient decay, can be modeled with a two-compartment model. However, for parameter-extraction in such a model, approximations are required regarding the relative sizes of the various model parameters. These approximations apply to certain cell types or experimental conditions and are not valid in the general case. In this paper, we present a general method for the extraction of the parameters in a two-compartment model without assumptions regarding the relative size of the parameters. All the passive electrical parameters of the two-compartment model are derived in terms of the available experimental data. The experimental data is obtained from a DC measurement (where the command potential is a hyperpolarizing DC voltage) and an AC measurement (where the command potential is a sinusoidal stimulus on a hyperpolarized DC potential) performed on the cell under test. Computer simulations are performed with a circuit simulator, XSPICE, to observe the effects of varying the two-compartment model parameters on the capacitive transients of the current response. Our general solution for the parameter-estimation of a two-compartment model may be used to model any neuron, which has a biexponential capacitive current decay. In addition, our model avoids the need for simplifying and perhaps erroneous approximations. Our equations may be easily implemented in hardware/software compensation schemes to correct the recorded currents for any series resistance or capacitive transient errors. Our general solution reduces to the results of previous researchers under their approximations. © 2002 Elsevier Science B.V. All rights reserved.

Keywords: Patch-clamping; Two-compartment; Whole-cell; Parameter-extraction; Modeling

Nomenclature

τ	single-compartment time constant (s)
τ_O	$C_D R_C R_D/(R_C+R_D)$ (s)
τ_1	$[(1/C_D)(1/R_M+1/R_C+1/R_S)]^{-1}$ (s)
τ_2	see Eq. (14) (s)
τ_3	two-compartment time constant (slow) (s)
τ_4	two-compartment time constant (fast) (s)
R_S	pipette resistance (ohm)
R_M	resistance of compartment M (ohm)
C_M	capacitance of compartment M (farad)
R_D	resistance of compartment D (ohm)
C_D	capacitance of compartment D (farad)
R_C	resistance connecting compartments M and D (ohm)
V_O	command potential (volts)

* Corresponding author. Tel.: +1-610-758-4518; fax: +1-610-758-4561
E-mail addresses: skp3@lehigh.edu (S. Pandey), mhw0@lehigh.edu (M.H. White).

PII: S0165-0270(02)00198-X

$V_1(t)$	potential at compartment M (volts)
$V_2(t)$	potential at compartment D (volts)
V_P	steady-state voltage component of $V_2(t)$ (s)
$i_1(t)$	total input current through the pipette (ampere)
i_{SS}	steady-state component of $i_1(t)$ (ampere)
A_O	single-compartment exponential-decay coefficient (ampere)
A_1	two-compartment current exponential-decay (slow) coefficient (ampere)
A_2	two-compartment current exponential-decay (fast) coefficient (ampere)
ξ	see Eq. (28) (s^{-2})
ω	operating frequency of the sinusoidal stimulus (radians/s)
$Y(\omega)$	single-compartment admittance at a frequency ω (ohm^{-1})
$A_R(\omega)$	real part of $Y(\omega)$ (ohm^{-1})
$B_R(\omega)$	imaginary part of $Y(\omega)$ (ohm^{-1})
R_{TOTAL}	single-compartment thevenin equivalent resistance (ohm)
R_{TOT}	two-compartment thevenin equivalent resistance (ohm)
$Y_{TOT}(\omega)$	two-compartment admittance at a frequency ω (ohm^{-1})
$Z_{TOT}(\omega)$	two-compartment impedance at a frequency ω (ohm)
$\alpha(\omega)$	real part of $Y_{TOT}(\omega)$ (ohm^{-1})
$\beta(\omega)$	imaginary part of $Y_{TOT}(\omega)$ (ohm^{-1})

1. Introduction

In most electrophysiological studies, whole-cell voltage-clamp techniques are an established method to measure ionic currents from single cells. An ideal voltage clamp has two functions: first, it imposes a command potential on the membrane such that the cell membrane potential is equal to the command potential and second, it measures the ionic current. In reality, there is considerable resistance to the flow of current through the pipette to the cytoplasm. As a result of this current flow, the membrane potential is not equal to the applied command potential. The signal response time (time constant) is essentially a function of the pipette resistance, the membrane resistance and capacitance. An estimation of these electrical components is needed to compensate for the series resistance and capacitive transient errors in a voltage-clamp experiment.

Compartmental models are often used to represent a cell's passive electrical properties, which provide a useful insight into the different cell conduction mechanisms. In the simplest case, a single-compartment model (Fig. 1) can be used to represent the electrical characteristics of small cells (longest dimension <100 μm). Here, the capacitive transient of the current response to a hyperpolarized voltage step (i.e. a negative step voltage relative to the intracellular medium) has a single-exponential decay time constant. Also, the membrane resistance is usually 50–100 times larger than the pipette resistance (5–10 MΩ). As such, the method of parameter-estimation in a single-compartment model becomes quite trivial and, over time, numerous methods have evolved for the extraction of these parameters. If we assume the membrane resistance is much larger than the pipette resistance, then all single-compartment model parameters can be estimated within reasonable accuracy (Sakmann and Neher, 1994). A more exact method of parameter-estimation involves admittance measurements (Lindau and Neher, 1988), where the model parameters can be expressed in terms of the real and imaginary components of the measured admittance. Also, the dynamic changes in passive cellular characteristics may be measured with phase-tracking techniques (Fidler and Fernandez, 1989) or by other dual-frequency measurement approaches (Donnelly, 1994). Computer simulations have been performed by Sala et al. to examine the sources of errors introduced by the single-compartment model parameters in single-electrode voltage-clamp experiments (Sala and Sala, 1994). Recently a method, which employs planar pipettes in silicon, was suggested to reduce noise sources in patch-clamping and for high-throughput screening (Pandey and White, 2001).

A single-compartment model cannot describe some cells. In neurons, such as the cerebellar Purkinje cells, the capacitive current response to a hyperpolarizing voltage pulse is a sum of two exponentials. These cells can be modeled satisfactorily with a two-compartment equivalent circuit. In a two-compartment model, the equivalent electrical circuit consists of two main compartments (soma and proximal dendrites on the one hand, distal dendrites on the other) connected by a resistance. In hippocampal pyramidal cells, three exponentials are needed to model the capacitive decay. In these instances, and many more complex cases, a cable analysis may be more appropriate than a multi-compartment model (Koch and Segev, 1989). The cable method for analyzing passive electrical data from neurons consists of decomposing the voltage response

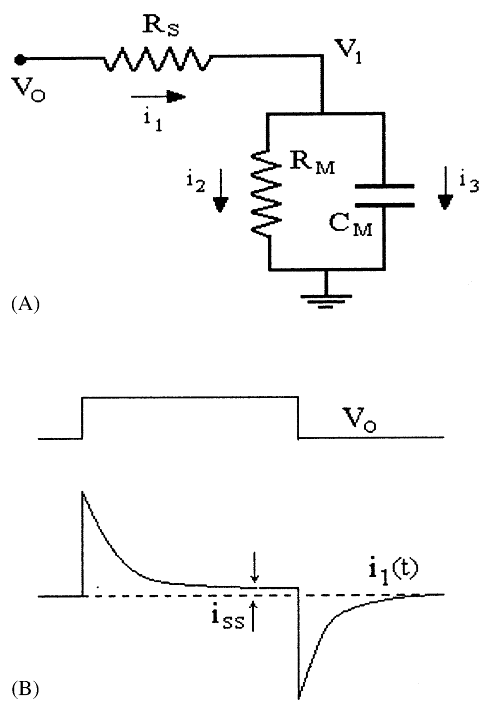

Fig. 1. (A) A single-compartment model showing the passive electrical equivalent circuit of a small cell. (B) The typical waveforms of the command voltage V_O and the recorded current $i_1(t)$ versus time.

of the cell into a series of exponential functions and substituting the time constants of these exponential functions into equations derived from cable theory (Rall et al., 1992). As an alternative to this traditional method of cable analysis, the method of 'integrals of transients' has been employed to analyze the passive electrical data from neurons (Engelhardt et al., 1998).

Yet, the simpler the compartmental model, the easier it becomes to estimate its model parameters (Roth and Hausser, 2001). Unfortunately, even in a two-compartment model, some approximations need to be made to simplify the model and thereby, ease the method of parameter-extraction. Llano et al. (1991) employed a two-compartment model to fit the capacitive transients of the excitatory currents from Purkinje cells as a sum of two exponentials. Llano et al. (1991) assumed the resistances in the proximal and distal compartments were very large compared with the other resistances in the equivalent circuit. The biexponential decay of capacitive transients from hippocampal cells was described using a two-compartment model by Mennerick et al. (1995) assuming the resistance of the distal compartment is very large. In another work, a simplified two-compartment model was used to extract the membrane properties of bipolar neurons, assuming very high resistances in the proximal and distal compartments (Mennerick et al., 1997). A recent work compared the various approximations made by previous authors while using a two-compartment model, summarizing the validity and limits of these approximations under different conditions (Nadeau and Lester, 2000).

The reliability of any parameter-extraction technique depends on the approximations made while extracting the model parameters and on the validation of such approximations for the given cell and the bandwidth of operation. Compensation circuitry, either included in the software/hardware of the patch-clamp setup, relies on the accuracy of these parameter-extraction techniques to compensate for the errors introduced by the circuit resistance and capacitance (Traynelis, 1998). In some cases, certain simplifying approximations regarding the size of the model parameters can be justified. But in other cases, especially when dealing with complex and larger cells, a more exact model for the estimation of the parameters is required. This points out the need for a general method of parameter-estimation in a two-compartment model, which is not subjected to over-simplifying approximations.

In this work, we present an exact, analytical method for the parameter-estimation of a two-compartment model. All the passive electrical parameters of the two-compartment model are derived based on the DC measurements (where the command potential is a DC hyperpolarizing voltage) and on AC measurements (where the command potential is a sinusoidal stimulus resting upon a DC hyperpolarizing voltage). Our equations are compared to those derived by previous authors and, under approximations used by these authors, we obtain the same results. Computer simulations are performed on a circuit simulator, XSPICE, to demonstrate the contributions of varying each model parameter on the capacitive transients of the current response.

2. Single-compartment model (a review)

We assume a reasonably small cell (<100 μm) with a membrane resistance R_M and a membrane capacitance C_M. The command voltage V_O is applied to the cell through a pipette with a series resistance of R_S. Fig. 1 shows the electrical equivalent circuit of the small cell, along with the voltage and current waveforms associated with the circuit. This equivalent circuit representation of a small cell is often used with patch-clamp techniques in electrophysiological experiments. We assume the cell membrane is isopotential and there are no voltage-dependent, active conductances. In small cells, the typical values of the single-compartment model parameters are $R_S = 10$ MΩ, $R_M = 1$ GΩ and $C_M = 15$–100 pF. In such cases, the assumption of $R_M >> R_S$ is valid and simplifies the model. We will describe briefly the standard equations of this single-compartment model, estimating the model parameters by making the assumption of $R_M >> R_S$. Next, we will review a more accurate method for the estimation of the single-compartment model parameters based on admittance measurements with no simplifying assumptions. We will extend this approach to a two-compartment model, which will provide a technique for the extraction of the two compartment model parameters. From Fig. 1(A), we derive the equations

$$V_1(t) = \frac{V_O \tau}{R_S C_M}\left(1 - \exp\left(-\frac{t}{\tau}\right)\right) \tag{1}$$

where

$$\tau = C_M\left(\frac{R_M R_S}{R_M + R_S}\right)$$

is the circuit time constant and the current is

$$i_1(t) = \frac{V_O}{R_S}\left(1 - \frac{\tau}{R_S C_M}\right) + \frac{V_O \tau}{R_S^2 C_M}\exp\left(-\frac{t}{\tau}\right) \tag{2}$$

The experimentally recorded current $i_1(t)$ has the form

$$i_1(t) = i_{SS} + A_O \exp(-t/\tau) \tag{3}$$

where i_{SS} is the steady state component of $i_1(t)$. Comparing Eq. (1) and Eq. (3) we have

$$i_{SS} = \frac{V_O}{R_S}\left(1 - \frac{\tau}{R_S C_M}\right) \quad \text{and} \quad A_O = \frac{V_O \tau}{R_S^2 C_M} \tag{4}$$

With the assumption $R_M >> R_S$, the model parameters can be written as (Sakmann and Neher, 1994)

$$R_M = \frac{V_O}{i_{SS}}, \quad R_S = \frac{V_O}{i_1(0)}, \quad C_M = \frac{\tau}{R_S} \tag{5}$$

Computer simulations of the single-compartment equivalent circuit are performed on XSPICE, a circuit simulator. Fig. 2(A) shows the effect of varying the series resistance on the capacitive transient of the current $i_1(t)$ under the application of a 10 mV command voltage step. The values of the model parameters are chosen as $R_M = 100$ MΩ, $C_M = 20$ pF and $R_S = 2$, 3.5 and 5 MΩ. We see the series resistance compensation is increased (i.e. as R_S is decreased), the time constant τ decreases and the value of $i_1(0)$ or A_O increases (according to Eq. (2)). In Fig. 2(B), the amplitude of the command voltage step is varied and its effect on the capacitive transient of the current $i_1(t)$ is observed. The values of the model parameters are $R_M = 100$ MΩ, $C_M = 20$ pF and $R_S = 2$ MΩ. In Fig. 2(B), we observe that even though the time constant is fixed ($\tau = 39$ μs), the current $i_1(0)$ or A_O increases with increasing magnitude of the command voltage V_O (according to Eq. (2)).

We now review a method of parameter estimation for a single-compartment model, which gives an exact solution for the model parameters, without simplifying assumptions (Lindau and Neher, 1988). In this technique, a sinusoidal voltage stimulus resting upon a hyperpolarized DC potential is applied as the command voltage. The magnitude and phase-shift of the resulting current sinusoid are analyzed with a phase-sensitive detector to give the real and imaginary current components. These current components divided by the stimulus voltage amplitude give the real and imaginary admittance values. Using this information, along with the information from the measured DC current, all the parameters of a single-compartment model can be exactly determined.

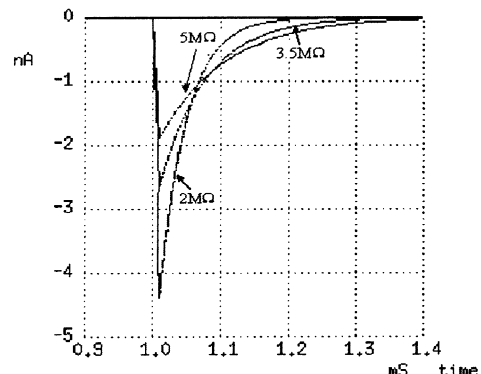

(A)

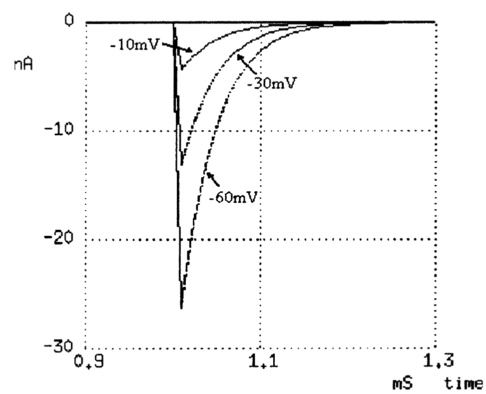

(B)

Fig. 2. (A) The effect of series resistance compensation on the capacitive transient of the current $i_1(t)$. The model parameters are $R_M = 100$ MΩ, $C_M = 20$ pF and $R_S = 2$, 3.5 and 5 MΩ. The fitting parameters for the single-exponential decay of the capacitive transients are: (a) for $R_S = 2$ MΩ, $\tau = 39$ μs, $A_O = 4.9$ nA, $i_{SS} = 0.098$ nA; (b) for $R_S = 3.5$ MΩ, $\tau = 68$ μs, $A_O = 2.7$ nA, $i_{SS} = 0.096$ nA; (c) for $R_S = 5$ MΩ, $\tau = 96$ μs, $A_O = 1.9$ nA, $i_{SS} = 0.095$ nA. (B) The effect of varying the command step voltage V_O on the capacitive transient of the current $i_1(t)$. The model parameters are $R_M = 100$ MΩ, $C_M = 20$ pF and $R_S = 2$ MΩ. The fitting parameters for the single-exponential decay of the capacitive transients are: $\tau = 39$ μs (a) for $V_O = -10$ mV, $A_O = 4.9$ nA, $i_{SS} = 0.098$ nA; (b) for $V_O = -30$ mV, $A_O = 14.7$ nA, $i_{SS} = 0.29$ nA; (c) for $V_O = -60$ mV, $A_O = 29.4$ nA, $i_{SS} = 0.59$ nA.

From Fig. 1(A), the net admittance is

$$Y(\omega) = A_R(\omega) + jB_R(\omega) = \frac{(1 + \omega^2 R_M R_P C_M^2) + j\omega R_M^2 C_M}{R_T(1 + \omega^2 R_P^2 C_M^2)} \tag{6}$$

where

$$R_T = R_M + R_S = \frac{V_O}{I_{DC}} \quad \text{and} \quad R_P = \frac{R_M R_S}{R_M + R_S} \tag{7}$$

With the experimental values of R_T, A_R and B_R, Eq. (6) and Eq. (7) give the model parameters as

$$\begin{aligned} R_S &= \frac{A_R - R_T^{-1}}{A_R^2 + B_R^2 - A_R R_T^{-1}}, \\ R_M &= \frac{R_T\{(A_R - R_T^{-1})^2 + B_R^2\}}{A_R^2 + B_R^2 - A_R R_T^{-1}}, \\ C_M &= \left(\frac{1}{\omega_C B_R}\right)\frac{(A_R^2 + B_R^2 - A_R R_T^{-1})^2}{(A_R - R_T^{-1})^2 + B_R^2} \end{aligned} \tag{8}$$

where $f_C = \omega_C/2\pi$ is the frequency of the applied sinusoid.

To estimate the three parameters R_S, R_M and C_M of the single-compartment model, at least three equations are needed. In the Lindau–Neher technique, the admittance measurement provides two equations and the DC current measurement provides the third equation needed to estimate all the model parameters. We use a similar methodology in the parameter-extraction of the two-compartment model. The current response $i_1(t)$ to a DC command voltage, together with the admittance measurements, will provide all the information needed to exactly estimate all the six parameters of the two-compartment model, as shown in the next section.

3. Two compartment model (DC measurements)

In this analysis, we assume a cell that can be modeled by an electrical equivalent circuit shown in Fig. 3. The DC step command voltage V_O is applied to the cell through a pipette with a series resistance R_S. The actual cell can be represented by two compartments: compartment M (for the soma and proximal dendrites) and compartment D (for the distal dendrites). A series resistance R_C connects the two compartments. Assuming the pipette capacitance is fully compensated, the following equations can be derived for the two-compartment model:

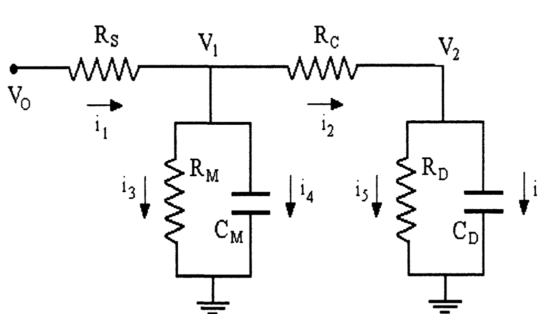

Fig. 3. Two-compartment model showing the two compartments: compartment M (for the soma and proximal dendrites) and compartment D (for the distal dendrites) connected by a resistance R_C. The pipette resistance is R_S and the command voltage stimulus is V_O.

$$\begin{aligned} &i_1 = (V_O - V_1)/R_S, \quad i_2 = (V_1 - V_2)/R_C, \quad i_3 = V_1/R_M, \\ &i_5 = V_2/R_D, \quad i_4 = C_M dV_1/dt, \quad i_6 = C_D dV_2/dt, \\ &i_1 - i_2 = i_3 + i_4, \quad i_2 = i_5 + i_6 \end{aligned} \tag{9}$$

From the above set of equations, we obtain two first-order differential equations

$$C_M \frac{dV_1(t)}{dt} + V_1(t)\left(\frac{1}{R_M} + \frac{1}{R_C} + \frac{1}{R_S}\right) = \frac{V_2(t)}{R_C} + \frac{V_O}{R_S} \tag{10}$$

$$C_D \frac{dV_2(t)}{dt} + V_2(t)\left(\frac{1}{R_C} + \frac{1}{R_D}\right) = \frac{V_1(t)}{R_C} \tag{11}$$

Eliminating $V_1(t)$ from these two differential equations gives a second-order non-homogeneous differential equation in $V_2(t)$ as

$$\frac{d^2V_2(t)}{dt^2} + \frac{dV_2(t)}{dt}\left[\frac{1}{\tau_O} + \frac{1}{\tau_1}\right] + V_2(t)\left[\frac{1}{\tau_O\tau_1} - \frac{1}{C_M C_D R_C^2}\right] = \frac{V_O}{C_M C_D R_C R_S} \tag{12}$$

where

$$\frac{1}{\tau_O} = \frac{1}{C_D}\left(\frac{1}{R_C} + \frac{1}{R_D}\right) \quad \text{and} \quad \frac{1}{\tau_1} = \frac{1}{C_M}\left(\frac{1}{R_M} + \frac{1}{R_C} + \frac{1}{R_S}\right) \tag{13}$$

The solution of such a differential equation is of the form: $V(t) = c_1 \exp(-t/\tau_3) + c_2 \exp(-t/\tau_4) + V_P$, where V_P is the particular solution of the above differential equation and the exponential terms are the solutions of the homogeneous differential equation. The constants c_1 and c_2 can be determined from the given initial conditions. For Eq. (12), the particular solution V_P is

$$V_P = \frac{V_O R_M \tau_2}{C_D(R_M R_S + R_M R_C + R_C R_S)}$$

where

$$\tau_2 = C_D\left[\frac{1}{R_D} + \frac{(R_S + R_M)}{R_M R_S + R_M R_C + R_C R_S}\right]^{-1} \tag{14}$$

The homogeneous solution of the differential Eq. (12) gives the two circuit time constants as

$$\frac{1}{\tau_3} = \left(\frac{1}{\tau_O\tau_1} - \frac{1}{R_C^2 C_M C_D}\right) \Big/ \left(\frac{1}{\tau_O} + \frac{1}{\tau_1}\right) \tag{15}$$

$$\frac{1}{\tau_4} = \left[\left(\frac{1}{\tau_O} + \frac{1}{\tau_1}\right)^2 - \left(\frac{1}{\tau_O\tau_1} - \frac{1}{R_C^2 C_M C_D}\right)\right] \Big/ \times \left(\frac{1}{\tau_O} + \frac{1}{\tau_1}\right) \tag{16}$$

We also have a relation between the two time constants as

$$\left(\frac{1}{\tau_4}-\frac{1}{\tau_3}\right)=\left(\frac{1}{\tau_O}+\frac{1}{\tau_1}\right) \tag{17}$$

The initial conditions of $V_2(0)=0$ and $V_1(0)=0$ give the general solutions of $V_1(t)$ and $V_2(t)$ as

$$\begin{aligned} V_2(t) &= \left(\frac{V_O R_M \tau_2}{C_D(R_M R_C + R_M R_S + R_C R_S)}\right) \\ &\quad\times\left[1+\left(\frac{\tau_3}{\tau_4-\tau_3}\right)\exp\left(-\frac{t}{\tau_3}\right) - \left(\frac{\tau_4}{\tau_4-\tau_3}\right)\exp\left(-\frac{t}{\tau_4}\right)\right] \end{aligned} \tag{18}$$

$$\begin{aligned} V_1(t) &= \left(\frac{V_O R_M R_C \tau_2}{\tau_O(R_M R_C + R_M R_S + R_C R_S)}\right) \\ &\quad\times\left[1+\left(\frac{\tau_3-\tau_O}{\tau_4-\tau_3}\right)\exp\left(-\frac{t}{\tau_3}\right) - \left(\frac{\tau_4-\tau_O}{\tau_4-\tau_3}\right)\exp\left(-\frac{t}{\tau_4}\right)\right] \end{aligned} \tag{19}$$

In the approximation of $C_M=0$ (Nadeau and Lester, 2000), we observe the time constants in Eq. (15) and Eq. (16) reduce to $\tau_3=\tau_2$ and $\tau_4=0$. If we place the values of these time constants into Eq. (18), then we will have the same result obtained by Nadeau and Lester (2000). The next section will provide additional validation of the above set of equations for the two-compartment model. Now, the experimentally recorded current $i_1(t)$ has the form

$$i_1(t)=i_{SS}+A_1\exp\left(-\frac{t}{\tau_3}\right)+A_2\exp\left(-\frac{t}{\tau_4}\right) \tag{20}$$

where i_{SS} is the steady-state current component of $i_1(t)$, while τ_3 (slow) and τ_4 (fast) are the two time constants of the biexponential capacitive transient. Fitting the experimental plot of $i_1(t)$ with Eq. (20) will provide the values of all the equation unknowns (i_{SS}, τ_3, τ_4, A_1, A_2). From the experimental plot of $i_1(t)$, the following parameters can be determined:

$$\begin{aligned} R_{TOT}&=\frac{V_O}{i_{SS}}, \quad R_S=\frac{V_O}{i_1(0)}=\frac{V_O}{A_1+A_2+i_{SS}}, \\ C_M&=-\frac{V_O}{R_S^2(di_1(0)/dt)}=\frac{\tau_3\tau_4(A_1+A_2+i_{SS})^2}{V_O(A_1\tau_4+A_2\tau_3)} \end{aligned} \tag{21}$$

Eq. (21) allows us to estimate the parameters R_S and C_M from the known values of the current parameters (i_{SS}, τ_3, τ_4, A_1, A_2) in Eq. (20). Also, from Fig. 3 and Eq. (21), R_M can be expressed in terms of R_{TOT}, R_S, R_C and R_D as

$$\frac{1}{R_{TOT}-R_S}=\frac{1}{R_M}+\frac{1}{R_C+R_D} =\frac{i_{SS}(A_1+A_2+i_{SS})}{V_O(A_1+A_2)} \tag{22}$$

Using the form of $i_1(t)$ from Eq. (20), the voltage $V_1(t)$ can be expressed as

$$V_1(t)=V_O-R_S\left[i_{SS}+A_1\exp\left(-\frac{t}{\tau_3}\right) +A_2\exp\left(-\frac{t}{\tau_4}\right)\right] \tag{23}$$

Comparing the two forms of voltage $V_1(t)$ from Eq. (19) and Eq. (23) gives the values of τ_O, τ_1 and τ_2 in terms of the known parameters as

$$\tau_O=\frac{C_D R_C R_D}{R_C+R_D}=\frac{A_1\tau_4+A_2\tau_3}{A_1+A_2} \tag{24}$$

$$\tau_1=\left(\frac{1}{\tau_4}-\frac{1}{\tau_3}-\frac{1}{\tau_O}\right)^{-1} \tag{25}$$

$$\tau_2=\frac{R_S C_M \tau_O}{V_O\tau_1}\ (V_O-i_{SS}R_S) \tag{26}$$

Now, from the expression of τ_3, the model parameter C_D can be expressed as

$$C_D^{-1}=R_C^2 C_M \xi$$

where

$$\xi=\left[\frac{1}{\tau_O\tau_1}-\frac{1}{\tau_3}\left(\frac{1}{\tau_4}-\frac{1}{\tau_3}\right)\right] \tag{27}$$

The relation between R_C and R_D can be found from Eq. (13) and Eq. (22) as

$$\frac{R_D}{R_C+R_D}=R_C\left(\frac{C_M}{\tau_1}-\frac{1}{R_S}-\frac{1}{R_{TOT}-R_S}\right) \tag{28}$$

We have shown the derivations of a two-compartment model based on DC measurements. Our objective is to express the model unknowns (R_S, R_M, R_C, R_D, C_M, C_D) in terms of the known parameters (i_{SS}, τ_3, τ_4, A_1, A_2) of the experimentally recorded current (Eq. (20)). We are able to extract some parameters (R_S, R_{TOT}, C_M, τ_o, τ_1, τ_2) in this process, but the other model unknowns (R_C, R_D, R_M, C_D) may only be expressed in terms of some interdependent equations. In the next section, we will continue with our derivations for the parameter-extraction of a two-compartment model, to express the 'still-unknown' model parameters in the form of independent equations.

4. Comparison with previous work

In our derivations until now, we have avoided making simplifying assumptions or approximations regarding the relative sizes of the circuit components. At this point, it is interesting to review the previous work on the two-compartment modeling. In these works, simplifying assumptions are made, which provides a unique solution to the equivalent circuit model based on DC measurements. If we apply these assumptions to our general set of equations, then our equations reduce to previous reported work.

Llano et al. (1991) uses the assumption of $R_M = \infty$, $R_D >> R_C$, R_S and $C_D >> C_M$ for modeling the currents of Purkinje cells. This simplifying assumption works well for determining the passive properties of Purkinje neurons. As will be shown below, the results in the reference (Llano et al., 1991) can be obtained from the general set of equations we have already derived for the two-compartment model. If we use the above assumption, then Eq. (13), Eq. (15) and Eq. (16) yield

$$\tau_O = C_D R_C, \quad \frac{1}{\tau_1} = \frac{1}{\tau_4} = \frac{1}{C_M}\left(\frac{1}{R_C} + \frac{1}{R_S}\right), \quad \tau_2 = \tau_3 = C_D(R_C + R_S) \tag{29}$$

Inserting Eq. (29) into Eq. (19) provides

$$V_1(t) = V_O\left[1 - \frac{R_S}{R_C + R_S}\exp\left(-\frac{t}{\tau_3}\right) + \frac{R_C}{R_C + R_S}\exp\left(-\frac{t}{\tau_4}\right)\right] \tag{30}$$

Comparing Eq. (23) with Eq. (31) gives

$$A_1 = \frac{V_O}{R_C + R_S} \quad \text{and} \quad A_2 = \frac{V_O R_C}{R_S^2 + R_S R_C} \tag{31}$$

Eq. (29) and Eq. (31) are sufficient to extract the model parameters as

$$C_D = \frac{\tau_3 A_1}{V_O} \quad C_M = \frac{\tau_4 (A_1 + A_2)^2}{A_2 V_O} \quad R_S = \frac{V_O}{A_1 + A_2} \quad R_C = \frac{A_2 V_O}{A_1(A_1 + A_2)} \tag{32}$$

The results obtained by Llano et al. (1991) are the same as those shown in Eq. (32). Computer simulations are performed on a two-compartment model with the assumption that $R_D >> R_S$, R_C; $R_M = \infty$ and $C_D >> C_M$ and the results are shown in Fig. 4. A 10 mV command potential is applied as the voltage stimulus V_O. Fig. 4(A) shows the effect of series resistance compensation on the capacitive transient of the current $i_1(t)$. The model parameters chosen are $C_M = 5$ pF, $C_D = 100$ pF, $R_C = 30$ MΩ and $R_S = 5$, 10 and 15 MΩ. From Eq. (31), we see the amplitude of A_2 (fast) is R_C/R_S times the amplitude of A_1 (slow). As the ratio of R_C/R_S is increased, the amplitude of A_2 also increases (evident from Fig. 4A). The amplitude of A_1, on the other hand, does not change significantly. Increasing the series resistance compensation decreases both the fast (τ_4) and the slow (τ_3) time constants. Fig. 4(B) shows the effect of varying R_C on the capacitive transient of the current $i_1(t)$ under the same assumption. The model parameters chosen are $C_M = 5$ pF, $C_D = 100$ pF, $R_S = 10$ MΩ and $R_C = 10$, 30 and 60 MΩ. In this case also, decreasing the value of R_C decreases both the fast (τ_4) and the slow (τ_3) time constants. However, the value of $i_1(0)$ is constant for varying values of R_C.

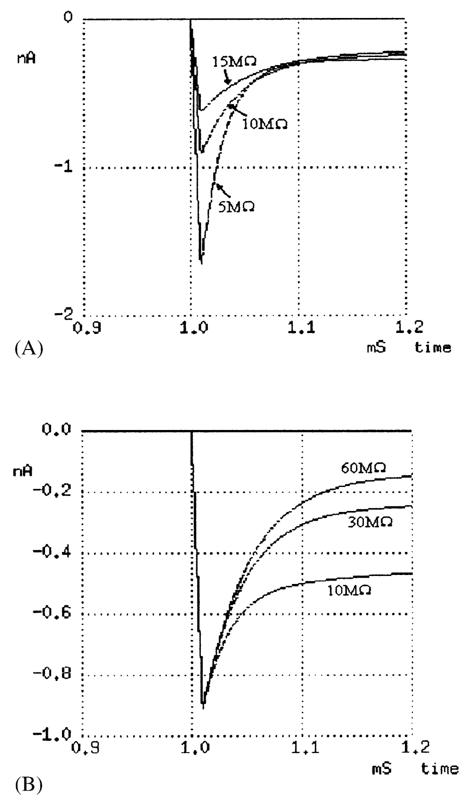

Fig. 4. (A) The effect of series resistance compensation on the capacitive transient of the current $i_1(t)$ under the assumption $R_D >> R_S$, R_C; $R_M = \infty$ and $C_D >> C_M$. A 10 mV command potential was applied as the voltage stimulus V_O. The model parameters chosen are $C_M = 5$ pF, $C_D = 100$ pF, $R_C = 30$ MΩ and $R_S = 5$, 10 and 15 MΩ. The fitting parameters for the biexponential decay of the capacitive transients are (a) for $R_S = 5$ MΩ, $\tau_3 = 3.5$ ms, $\tau_4 = 21.4$ μs, $A_1 = 0.28$ nA, $A_2 = 1.7$ nA; (b) for $R_S = 10$ MΩ, $\tau_3 = 4$ ms, $\tau_4 = 37.5$ μs, $A_1 = 0.25$ nA, $A_2 = 0.75$ nA; (c) for $R_S = 15$ MΩ, $\tau_3 = 4.5$ ms, $\tau_4 = 50$ μs, $A_1 = 0.22$ nA, $A_2 = 0.44$ nA. (B) The effect of varying R_C on the capacitive transient of the current $i_1(t)$ under the same assumption. The model parameters chosen are $C_M = 5$ pF, $C_D = 100$ pF, $R_S = 10$ MΩ and $R_C = 10$, 30 and 60 MΩ. The fitting parameters for the biexponential decay of the capacitive transients are (a) for $R_C = 10$ MΩ, $\tau_3 = 2$ ms, $\tau_4 = 25$ μs, $A_1 = 0.5$ nA, $A_2 = 0.5$ nA; (b) for $R_C = 30$ MΩ, $\tau_3 = 4$ ms, $\tau_4 = 37.5$ μs, $A_1 = 0.25$ nA, $A_2 = 0.75$ nA; (c) for $R_C = 60$ MΩ, $\tau_3 = 7$ ms, $\tau_4 = 43$ μs, $A_1 = 0.14$ nA, $A_2 = 0.86$ nA.

Mennerick et al. (1995) use the assumption $R_D >> R_M$ for modeling the passive properties of hippocampal neurons. Single-exponential fits are usually inadequate to describe the decay of current transients from these hippocampal neurons, but biexponential decays provided an adequate description of the data. The biexponential decay of capacitive transients indicates the passive membrane properties may be described adequately with a two-compartment equivalent circuit model. As shown below, with this assumption in our general set of equations, we obtain the same results as reported in the literature (Mennerick et al., 1995).

From Eq. (13) and Eq. (24) we have

$$\tau_O = R_C C_D = \frac{A_1\tau_4 + A_2\tau_3}{A_1 + A_2} \tag{33}$$

and with Eq. (21) and Eq. (22),

$$R_S = \frac{V_O}{A_1 + A_2 + i_{SS}}, \quad \frac{1}{R_M} = \frac{i_{SS}(A_1 + A_2 + i_{SS})}{V_O(A_1 + A_2)}, \quad C_M = \frac{\tau_3\tau_4(A_1 + A_2 + i_{SS})^2}{V_O(A_1\tau_4 + A_2\tau_3)} \tag{34}$$

Also, with Eq. (28) and Eq. (34),

$$R_C = \frac{(A_1 + A_2)(A_1\tau_4 + A_2\tau_3)^2 V_O}{A_1A_2(A_1 + A_2 + i_{SS})^2(\tau_4 - \tau_3)^2} \quad \text{and} \quad C_D = \left(\frac{1}{R_C}\right)\frac{A_1\tau_4 + A_2\tau_3}{A_1 + A_2} \tag{35}$$

5. Two-compartment model (admittance measurements)

A common method for measuring changes in membrane capacitances of small cells utilizes a sinusoidal voltage stimulus. The membrane capacitance is measured as a function of the real and imaginary admittance of the cell for the case of a single-compartment model. In this instance, this scheme is extended for a two-compartment model to help extract the remaining model parameters. If the AC admittance of the two-compartment model is $Y_{TOT}(\omega) = 1/Z_{TOT}(\omega) = \alpha(\omega) + j\beta(\omega)$, then from Fig. 3 we have

$$\frac{1}{Z_{TOT}(\omega) - R_S} = \frac{1}{R_M} + j\omega C_M + \frac{1 + j\omega C_D R_D}{R_C + R_D + j\omega C_D R_C R_D} \tag{36}$$

which can be written as

$$\frac{\{\alpha - R_S(\alpha^2 + \beta^2)\} + j\beta}{\{(1 - \alpha R_S)^2 + (\beta R_S)^2\}} = \frac{1}{R_M} + j\omega C_M + \frac{R_C + j\omega\tau_O(R_C + R_D)}{R_C(R_C + R_D)(1 + j\omega\tau_O)} \tag{37}$$

Equating the real parts of the Eq. (37) and using Eq. (13), we find

$$\frac{1}{(R_C + R_D)(1 + \omega^2\tau_O^2)} = \frac{1}{R_C(1 + \omega^2\tau_O^2)} + \frac{1}{R_S} - \frac{C_M}{\tau_1} + \frac{\{\alpha - R_S(\alpha^2 + \beta^2)\}}{\{(1 - \alpha R_S)^2 + (\beta R_S)^2\}} \tag{38}$$

Inserting Eq. (13), Eq. (27) and Eq. (38) into Eq. (28) gives

$$\left[\frac{1}{R_C} + (1 + \omega^2\tau_O^2) \times \left\{\frac{1}{R_S} - \frac{C_M}{\tau_1} + \frac{\{\alpha - R_S(\alpha^2 + \beta^2)\}}{\{(1 - \alpha R_S)^2 + (\beta R_S)^2\}}\right\}\right] = \left(\frac{1}{\tau_O C_M R_C \xi} - 1\right)\left\{\frac{C_M}{\tau_1} - \frac{1}{R_S} - \frac{1}{R_{TOT} - R_S}\right\} \tag{39}$$

From Eq. (39), R_C can be expressed as

$$\frac{1}{R_C} = \frac{\left[\left\{\frac{(1 + \omega^2\tau_O^2)\{\alpha - R_S(\alpha^2 + \beta^2)\}}{\{(1 - \alpha R_S)^2 + (\beta R_S)^2\}}\right\} - \omega^2\tau_O^2\left\{\frac{C_M}{\tau_1} - \frac{1}{R_S}\right\} - \frac{1}{R_{TOT} - R_S}\right]}{\left\{\frac{1}{\tau_O C_M \xi}\left(\frac{C_M}{\tau_1} - \frac{1}{R_S} - \frac{1}{R_{TOT} - R_S}\right) - 1\right\}} \tag{40}$$

And from the expression $C_D^{-1} = R_C^2 C_M \xi$, we have

$$\frac{1}{C_D} = \left[\frac{\left\{\frac{1}{\tau_O\sqrt{C_M\xi}}\left(\frac{C_M}{\tau_1} - \frac{1}{R_S} - \frac{1}{R_{TOT} - R_S}\right) - \sqrt{C_M\xi}\right\}}{\left\{\frac{(1 + \omega^2\tau_O^2)\{\alpha - R_S(\alpha^2 + \beta^2)\}}{\{(1 - \alpha R_S)^2 + (\beta R_S)^2\}}\right\} - \omega^2\tau_O^2\left\{\frac{C_M}{\tau_1} - \frac{1}{R_S}\right\} - \frac{1}{R_{TOT} - R_S}}\right]^2 \tag{41}$$

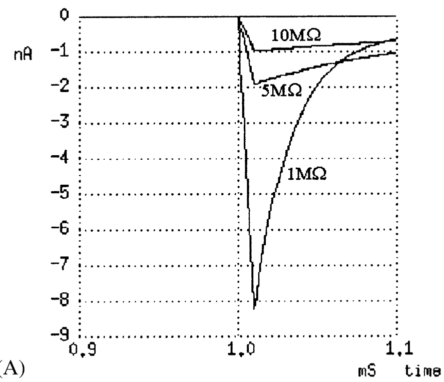

(A)

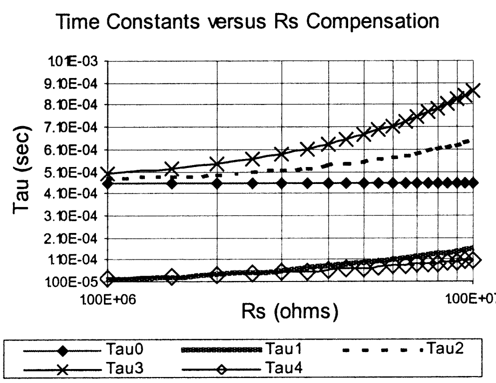

(B)

Fig. 5. (A) The effect of series resistance compensation on the capacitive transient of the current $i_1(t)$ in a two-compartment model (with no approximations). The model parameters chosen are $C_M = 25$ pF, $C_D = 25$ pF, $R_C = 20$ MΩ, $R_M = R_D = 200$ MΩ and $R_S = 1$, 5 and 10 MΩ. The fitting parameters for the biexponential decay of the capacitive transients are (a) for $R_S = 1$ MΩ, $\tau_3 = 0.5$ ms, $\tau_4 = 21.5$ μs, $A_1 = 0.94$ nA, $A_2 = 9$ nA, $i_{SS} = 0.095$ nA; (b) for $R_S = 5$ MΩ, $\tau_3 = 0.67$ ms, $\tau_4 = 72$ μs, $A_1 = 0.7$ nA, $A_2 = 1.2$ nA, $i_{SS} = 0.091$ nA; (c) for $R_S = 10$ MΩ, $\tau_3 = 0.87$ ms, $\tau_4 = 104$ μs, $A_1 = 0.5$ nA, $A_2 = 0.42$ nA, $i_{SS} = 0.087$ nA. (B) Plots the various values of τ_O, τ_1, τ_2, τ_3 and τ_4 (as defined by Eqs. (13)–(16)) as a function of the series resistance compensation. The model parameters are chosen as $C_M = 25$ pF, $C_D = 25$ pF, $R_C = 20$ MΩ and $R_M = R_D = 200$ MΩ. The range of the values of the other fitting parameters are $A_1 = 0.5$–0.94 nA, $A_2 = 0.42$–9.0 nA, $i_{SS} = 0.087$–0.095 nA.

Finally, we have

$$\frac{1}{R_D} = \frac{1}{R_C}\left(\frac{1}{R_C C_M \xi \tau_O} - 1\right) \quad \text{and} \qquad (42)$$

$$\frac{1}{R_M} = \frac{1}{R_{TOT} - R_S} - \frac{1}{R_C + R_D}$$

From the results obtained in previous sections, all the six two-compartment model parameters (R_C, R_D, R_M, R_S, C_M, C_D) are independently expressed in terms of the known parameters (i_{SS}, τ_3, τ_4, A_1, A_2) of the current $i_1(t)$ expression (Eq. (20)) and the known parameters ($\alpha(\omega)$, $\beta(\omega)$, ω) of the admittance measurements. A flowchart summarizing the steps for the extraction of the model parameters is shown at the end of the next section as

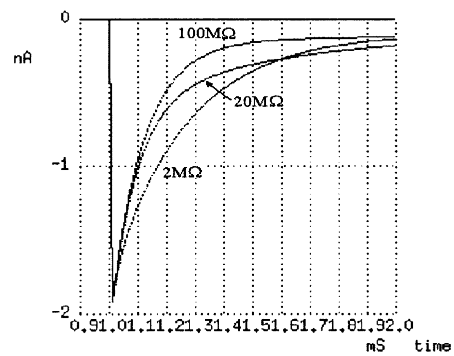

(A)

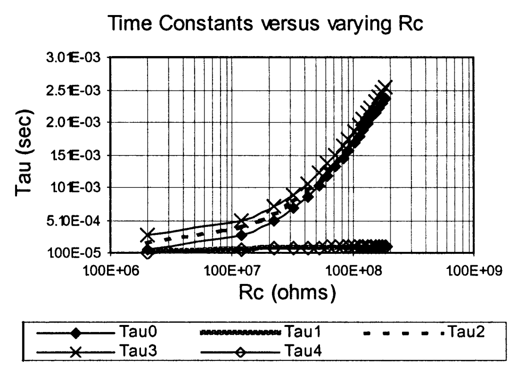

(B)

Fig. 6. (A) The effect of varying R_C on the capacitive transient of the current $i_1(t)$ in a two-compartment model (with no approximations). The model parameters chosen are $C_M = 25$ pF, $C_D = 25$ pF, $R_S = 5$ MΩ, $R_M = R_D = 200$ MΩ and $R_C = 2$, 20 and 100 MΩ. The fitting parameters for the biexponential decay of the capacitive transients are (a) for $R_C = 2$ MΩ, $\tau_3 = 0.3$ ms, $\tau_4 = 19.3$ μs, $A_1 = 1.7$ nA, $A_2 = 0.22$ nA, $i_{SS} = 0.095$ nA; (b) for $R_C = 20$ MΩ, $\tau_3 = 0.67$ ms, $\tau_4 = 72$ μs, $A_1 = 0.69$ nA, $A_2 = 1.22$ nA, $i_{SS} = 0.09$ nA; (c) for $R_C = 100$ MΩ, $\tau_3 = 1.84$ ms, $\tau_4 = 103$ μs, $A_1 = 0.19$ nA, $A_2 = 1.73$ nA, $i_{SS} = 0.08$ nA. (B) Plots the various values of τ_O, τ_1, τ_2, τ_3 and τ_4 (as defined by Eqs. (13)–(16)) as a function of R_C. The model parameters are chosen as $C_M = 25$ pF, $C_D = 25$ pF, $R_S = 5$ MΩ and $R_M = R_D = 200$ MΩ. The range of the values of the other fitting parameters $A_1 = 0.12$–1.7 nA, $A_2 = 0.22$–1.8 nA, $i_{SS} = 0.073$–0.095 nA.

Fig. 11. Such an algorithm can be easily implemented in software, which takes (as input) the DC and AC measurement results and gives (as output) the values of the model parameters.

6. Two-compartment model (simulation results)

Computer simulations of the two-compartment model, based on our general parameter-extraction method, were performed on XSPICE. The effect of varying the series resistance compensation on the two-compartment model current response is shown in Fig. 5. The model parameters chosen are $C_M = 25$ pF, $C_D = 25$ pF, $R_C = 20$ MΩ, $R_M = R_D = 200$ MΩ and $R_S = 1$, 5 and 10 MΩ. Fig. 5(A) shows the effect of series resistance compensation on the capacitive transient of the current $i_1(t)$ in a two-compartment model. From $R_S = 1$ MΩ to

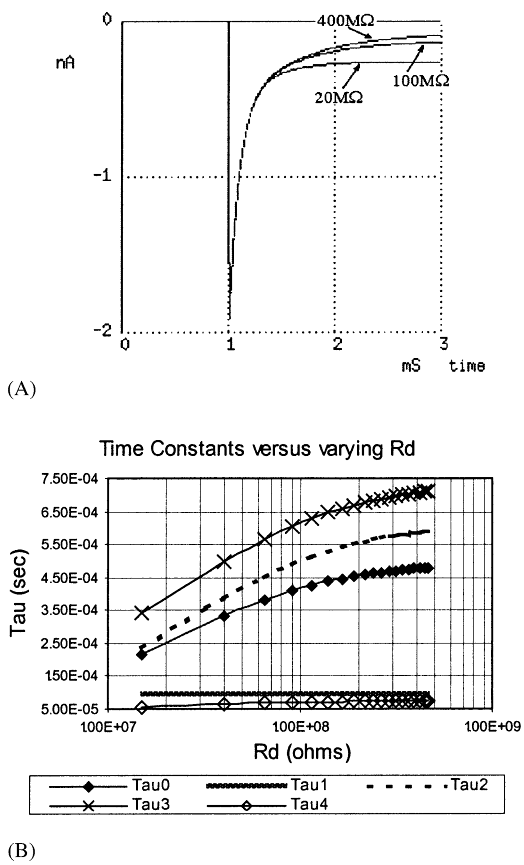

Fig. 7. (A) The effect of varying R_D on the capacitive transient of the current $i_1(t)$ in a two-compartment model (with no approximations). The model parameters chosen are $C_M = 25$ pF, $C_D = 25$ pF, $R_S = 5$ MΩ, $R_M = 200$ MΩ, $R_C = 20$ MΩ and $R_D = 20$, 100 and 400 MΩ. The fitting parameters for the biexponential decay of the capacitive transients are (a) for $R_D = 20$ MΩ, $\tau_3 = 0.39$ ms, $\tau_4 = 60$ µs, $A_1 = 0.725$ nA, $A_2 = 1.02$ nA, $i_{SS} = 0.26$ nA; (b) for $R_D = 100$ MΩ, $\tau_3 = 0.615$ ms, $\tau_4 = 70.3$ µs, $A_1 = 0.68$ nA, $A_2 = 1.2$ nA, $i_{SS} = 0.125$ nA; (c) for $R_D = 400$ MΩ, $\tau_3 = 0.71$ ms, $\tau_4 = 73$ µs, $A_1 = 0.7$ nA, $A_2 = 1.23$ nA, $i_{SS} = 0.07$ nA. (B) Plots the various values of τ_O, τ_1, τ_2, τ_3 and τ_4 (as defined by Eqs. (13)–(16)) as a function of R_D. The model parameters are chosen as $C_M = 25$ pF, $C_D = 25$ pF, $R_S = 5$ MΩ and $R_M = 200$ MΩ. The range of the values of the other fitting parameters $A_1 = 0.7$–0.76 nA, $A_2 = 0.95$–1.23 nA, $i_{SS} = 0.07$–0.3 nA.

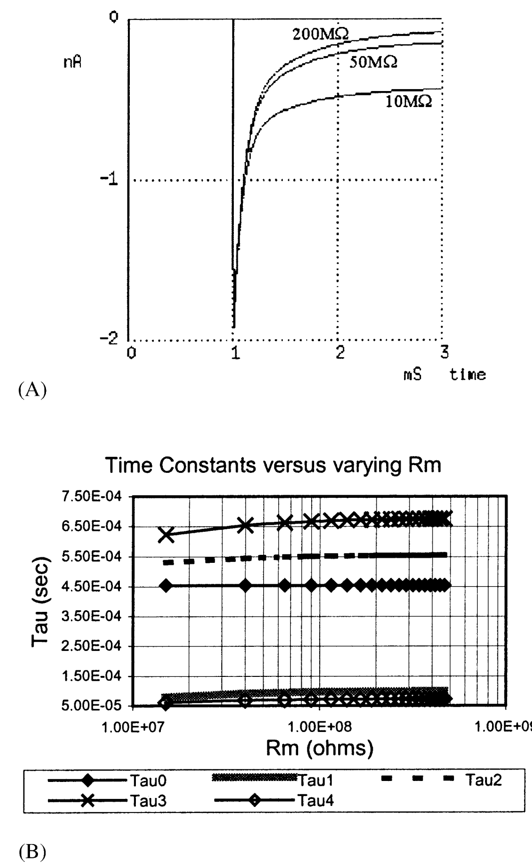

Fig. 8. (A) The effect of varying R_M on the capacitive transient of the current $i_1(t)$ in a two-compartment model (with no approximations). The model parameters chosen are $C_M = 25$ pF, $C_D = 25$ pF, $R_S = 5$ MΩ, $R_D = 200$ MΩ, $R_C = 20$ MΩ and $R_M = 10$, 50 and 200 MΩ. The fitting parameters for the biexponential decay of the capacitive transients are (a) for $R_M = 10$ MΩ, $\tau_3 = 0.6$ ms, $\tau_4 = 56$ µs, $A_1 = 0.46$ nA, $A_2 = 1.05$ nA, $i_{SS} = 0.7$ nA; (b) for $R_M = 50$ MΩ, $\tau_3 = 0.66$ ms, $\tau_4 = 69$ µs, $A_1 = 0.62$ nA, $A_2 = 1.2$ nA, $i_{SS} = 0.22$ nA; (c) for $R_M = 200$ MΩ, $\tau_3 = 0.67$ ms, $\tau_4 = 72$ µs, $A_1 = 0.7$ nA, $A_2 = 1.22$ nA, $i_{SS} = 0.09$ nA. (B) Plots the various values of τ_O, τ_1, τ_2, τ_3 and τ_4 (as defined by Eqs. (13)–(16)) as a function of R_M. The model parameters are chosen as $C_M = 25$ pF, $C_D = 25$ pF, $R_S = 5$ MΩ and $R_D = 200$ MΩ. The range of the values of the other fitting parameters $A_1 = 0.44$–0.71 nA, $A_2 = 1.03$–1.23 nA, $i_{SS} = 0.07$–0.53 nA.

$R_S = 10$ MΩ, the increase in τ_3 (slow) is not so significant (0.5–0.87 ms) compared to the increase in τ_4 (fast) (21.5–104 µs). Also, the value of $i_1(0)$ is very sensitive to changes in R_S. Fig. 5(B) plots the various values of τ_O, τ_1, τ_2, τ_3 and τ_4 (as defined by Eqs. (13)–(16)) as a function of the series resistance compensation. According to Eq. (13), τ_O is relatively independent of R_S, as shown in Fig. 5. It should be noted here that fast exponential decay time constant of the capacitive transient is τ_4, while the slow exponential decay time constant is τ_3. The variables τ_1 (fast) and τ_2 (slow) represent the two time constants for a two-compartment model under the approximation of $R_M = \infty$, $R_D >> R_C$, R_S and $C_D >> C_M$ (Llano et al., 1991). As seen in Fig. 5(B), the time constants τ_1 and τ_4 are close to each other, but the difference between the time constants τ_2 and τ_3 increases with increasing values of R_S. This shows the limitation of using an approximated two-compartment model with a high series resistance. In addition, the difference between the time constants τ_2 and τ_3 increases with an increasing value of the connecting resistance R_C. Finally, both time constants of the general two-compartment model, τ_3 and τ_4, depend and change with varying values of R_S. This is in contrast to the finite-cable model, where changing R_S affects only the first, faster time constant and leaves the slower one unchanged.

Fig. 6 shows the effect of varying R_C on the current response of a two-compartment model. Fig. 6(A) shows the effect of varying R_C on the capacitive transient of the current $i_1(t)$. The model parameters chosen are $C_M = 25$

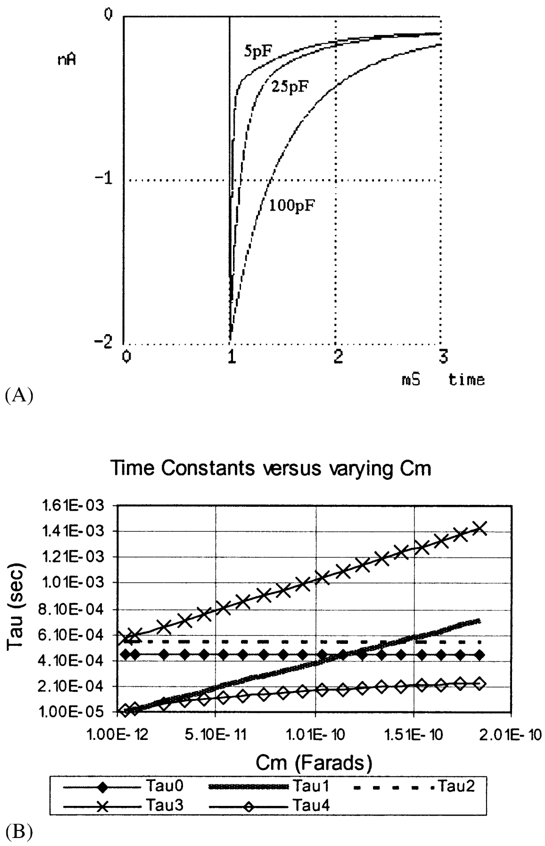

Fig. 9. (A) The effect of varying C_M on the capacitive transient of the current $i_1(t)$ in a two-compartment model (with no approximations). The model parameters chosen are $C_D = 25$ pF, $R_S = 5$ MΩ, $R_M = R_D = 200$ MΩ, $R_C = 20$ MΩ and $C_M = 5$, 25 and 100 pF. The fitting parameters for the biexponential decay of the capacitive transients are (a) for $C_M = 5$ pF, $\tau_3 = 0.6$ ms, $\tau_4 = 18$ μs, $A_1 = 0.42$ nA, $A_2 = 1.5$ nA, $i_{SS} = 0.09$ nA; (b) for $C_M = 25$ pF, $\tau_3 = 0.67$ ms, $\tau_4 = 72$ μs, $A_1 = 0.7$ nA, $A_2 = 1.22$ nA, $i_{SS} = 0.09$ nA; (c) for $C_M = 100$ pF, $\tau_3 = 1.03$ ms, $\tau_4 = 175$ μs, $A_1 = 1.3$ nA, $A_2 = 0.63$ nA, $i_{SS} = 0.09$ nA. (B) Plots the various values of τ_O, τ_1, τ_2, τ_3 and τ_4 (as defined by Eqs. (13)–(16)) as a function of C_M. The model parameters are chosen as $C_D = 25$ pF, $R_S = 5$ MΩ and $R_M = R_D = 200$ MΩ. The range of the values of the other fitting parameters are $A_1 = 0.42$–1.6 nA, $A_2 = 0.35$–1.5 nA, $i_{SS} = 0.09$ nA.

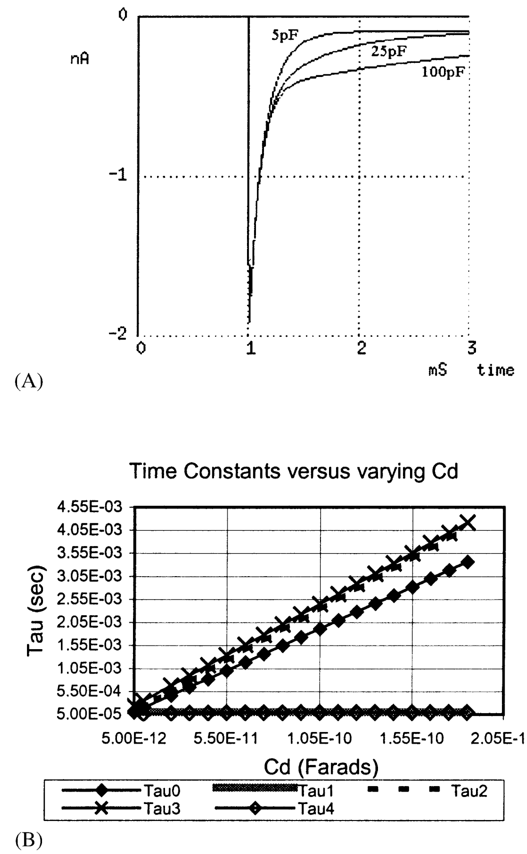

Fig. 10. (A) The effect of varying C_D on the capacitive transient of the current $i_1(t)$ in a two-compartment model (with no approximations). The model parameters chosen are $C_M = 25$ pF, $R_S = 5$ MΩ, $R_M = R_D = 200$ MΩ, $R_C = 20$ MΩ and $C_D = 5$, 25 and 100 pF. The fitting parameters for the biexponential decay of the capacitive transients are (a) for $C_D = 5$ pF, $\tau_3 = 0.23$ ms, $\tau_4 = 39$ μs, $A_1 = 1.4$ nA, $A_2 = 0.52$ nA, $i_{SS} = 0.09$ nA; (b) for $C_D = 25$ pF, $\tau_3 = 0.67$ ms, $\tau_4 = 72$ μs, $A_1 = 0.7$ nA, $A_2 = 1.22$ nA, $i_{SS} = 0.09$ nA; (c) for $C_D = 100$ pF, $\tau_3 = 2.33$ ms, $\tau_4 = 90$ μs, $A_1 = 0.44$ nA, $A_2 = 1.47$ nA, $i_{SS} = 0.09$ nA. (B) Plots the various values of τ_O, τ_1, τ_2, τ_3 and τ_4 (as defined by Eqs. (13)–(16)) as a function of C_D. The model parameters are chosen as $C_M = 25$ pF, $R_S = 5$ MΩ, $R_M = R_D = 200$ MΩ and $R_C = 20$ MΩ. The range of the values of the other fitting parameters are $A_1 = 0.39$–1.39 nA, $A_2 = 0.52$–1.52 nA, $i_{SS} = 0.09$ nA.

pF, $C_D = 25$ pF, $R_S = 5$ MΩ, $R_M = R_D = 200$ MΩ and $R_C = 2$, 20 and 100 MΩ. Fig. 6(B) plots the various values of τ_O, τ_1, τ_2, τ_3 and τ_4 (as defined by Eqs. (13)–(16)) as a function of R_C. The model parameters chosen in this case are the same as those for Fig. 6(A). From both the plots, the slow time constant τ_3 is very sensitive to increases in the value of R_C, whereas the other time constant τ_4 is relatively constant with any changes in the value of R_C. Also, the difference between τ_2 and τ_3 becomes smaller with increasing values of R_C. This shows that the approximation of $C_M = 0$ by Nadeau and Lester (2000) is valid only for larger values of R_C where the difference between the two time constants, τ_3 and τ_4, is large.

Fig. 7 shows the effect of varying R_D on the current response of a two-compartment model. The model parameters chosen are $C_M = 25$ pF, $C_D = 25$ pF, $R_S = 5$ MΩ, $R_M = 200$ MΩ, $R_C = 20$ MΩ and $R_D = 20$, 100 and 400 MΩ. Fig. 7(A) shows the effect of varying R_D on the capacitive transient of the current $i_1(t)$. Fig. 7(B) plots the various values of τ_O, τ_1, τ_2, τ_3 and τ_4 as a function of R_D, choosing the same values of the model parameters. Similar to Fig. 6, we see a strong dependence of the slow time constant τ_3 on the varying values of R_D, while the fast time constant τ_4 is relatively independent of such changes in R_D. The difference between τ_2 and τ_3 is more pronounced for smaller values of R_C.

Fig. 8 shows the effect of varying R_M on the current response of a two-compartment model. The model parameters chosen are $C_M = 25$ pF, $C_D = 25$ pF, $R_S = 5$ MΩ, $R_D = 200$ MΩ, $R_C = 20$ MΩ and $R_M = 10$, 50 and 200 MΩ. Fig. 8(A) shows how the capacitive transient of

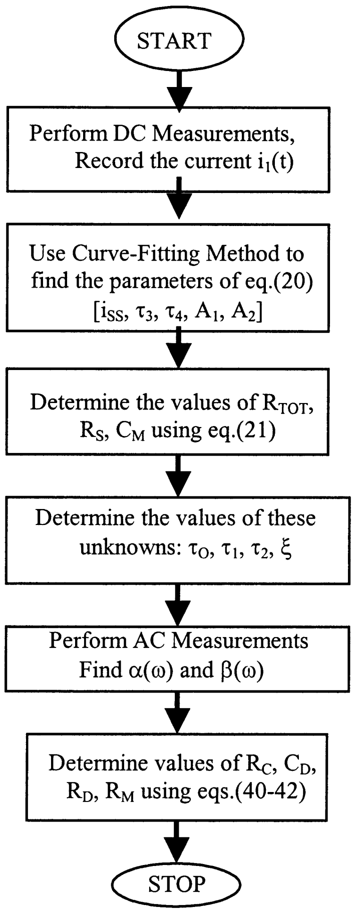

Fig. 11. A flowchart to summarize the steps for the parameter-extraction of a two-compartment model using the algorithm described in this work.

the current $i_1(t)$ varies with changing R_M. Fig. 8(B) plots the various values of τ_O, τ_1, τ_2, τ_3 and τ_4 as a function of R_M, choosing the same values of the model parameters. As seen in Fig. 8, the time constants τ_1, τ_2, τ_3 and τ_4 exhibit less dependence on the varying values of R_M. Yet, there is significant difference between the curves of τ_2 and τ_3, suggesting that for relatively smaller values of R_C, the more accurate time constant (slow) is τ_3 and not τ_2 (which is the slow time constant under the approximation made by Llano et al. (1991)).

Fig. 9 shows the effect of varying C_M on the current response of a two-compartment model. The model parameters chosen are $C_D = 25$ pF, $R_S = 5$ MΩ, $R_M = R_D = 200$ MΩ, $R_C = 20$ MΩ and $C_M = 5$, 25 and 100 pF. Fig. 9(A) shows the effect of varying C_M on the capacitive transient of the current $i_1(t)$. Fig. 9(B) plots the various values of τ_O, τ_1, τ_2, τ_3 and τ_4 as a function of C_M, choosing the same values of the model parameters. As seen in Fig. 9, both the time constants τ_3 and τ_4 vary with changing values of C_M; the dependence of the slow time constant τ_3 on such changes being much more significant. The curve of τ_2 is relatively independent of varying C_M because it was the slow time constant for the case where $C_M = 0$ in a two-compartment model (Llano et al., 1991; Nadeau and Lester, 2000). In this case, there is noticeable error involved in the computation of the time constants if approximations are made in the two-compartment model. This error becomes more and more significant as the value of C_M increases.

Fig. 10 shows the effect of varying C_D on the current response of a two-compartment model. The model parameters chosen are $C_M = 25$ pF, $R_S = 5$ MΩ, $R_M = R_D = 200$ MΩ, $R_C = 20$ MΩ and $C_D = 5$, 25 and 100 pF. Fig. 10(A) shows the effect of varying C_D on the capacitive transient of the current $i_1(t)$. Fig. 10(B) plots the various values of τ_O, τ_1, τ_2, τ_3 and τ_4 as a function of C_D, choosing the same values of the model parameters. As seen from Fig. 10, the fast time constant τ_4 is relatively constant with changing values of C_D, while the slow time constant τ_3 shows a sharp, linear increase with increasing values of C_D. The curves of τ_2 and τ_3 follow each other closely and so does the curves of τ_1 and τ_4. As such, making an approximation about the relative size of C_D does not introduce any significant error in the computation of the time constants.

7. Conclusion

In summary, we have derived a general solution for the parameter-estimation of a two-compartment model. With simplifying approximations, used by previous authors, our derivations are consistent with their results. The computer simulation results of the general two-compartment model give valuable insight into the role of each model parameter in the current response of such an equivalent circuit. We have compared the various time constants (those from approximated models and those from our general model) under the effects of varying model parameters. The difference between the time constants (related to the approximated models and our general model) increases with decreasing values of the connecting resistance R_C. As seen from the simulations, each of the model parameters has a unique effect on the variation of the different time constants. Employing an approximated model may not reveal the exact values of the model parameters, which are calculated from these time constants. The general method for the extraction of parameters is not limited by any simplifying approximations and so gives an exact solution of the two-compartment model.

Acknowledgements

The funding for this project was provided by National Science Foundation (ECS-0086178; Electronic DNA Sequencing with Ion Channel Research). S. Pandey is also supported by a Sherman Fairchild Graduate Fellowship.

References

Donnelly DF. A novel method for the rapid measurement of membrane resistance, capacitance, and access resistance. J Biophys 1994;66:873–7.

Engelhardt JK, Morales FR, Chase MH. An alternative method for the analysis of neuron passive electrical data which uses integrals of voltage transients. J Neurosci Methods 1998;81:131–8.

Fidler N, Fernandez JM. Phase tracking: an improved phase detection technique for cell membrane capacitance measurements. J Biophys 1989;56:1153–62.

Koch C, Segev I. Methods in Neuronal Modeling. USA: MIT Press, 1989:63–96.

Lindau M, Neher E. Patch-clamp techniques for time-resolved capacitance measurements in single cells. Pflugers Arch 1988;411:137–46.

Llano I, Marty A, Armstrong CM, Konnerth A. Synaptic- and agonist-induced excitory currents of Purkinje cells in rat cerebellar slices. J Physiol (Lond) 1991;434:183–213.

Mennerick S, Que J, Benz A, Zorumski CF. Passive and synaptic properties of hippocampal neurons grown in microcultures and in mass cultures. J Neurophysiol 1995;73:320–32.

Mennerick S, Zenisek D, Matthews G. Static and dynamic membrane properties of large-terminal bipolar cells from goldfish retina: experimental test of a compartment model. J Neurophysiol 1997;78:51–62.

Nadeau H, Lester HA. Two-compartment model for whole-cell data analysis and transient compensation. J Neurosci Methods 2000;99:25–35.

Pandey S, White M. An integrated planar patch-clamp system. ISDRS Proceedings 2001;10:170–73.

Rall W, Burke RE, Holmes WR, Jack JJB, Redman SJ, Segev I. Matching dendritic neuron models to experimental data. Physiol Rev 1992;72:S159–89.

Roth A, Hausser M. Compartmental models of rat cerebellar Purkinje cells based on simultaneous somatic and dendritic patch-clamp recordings. J Physiol (Lond) 2001;535:445–72.

Sakmann B, Neher E. Tight-Seal Whole-Cell Recording, Single-Channel Recording. New York: Plenum Press, 1994:31–51.

Sala F, Sala S. Sources of errors in different single-electrode voltage-clamp techniques: a computer simulation study. J Neurosci Methods 1994;53:189–97.

Traynelis SF. Software-based correction of single-compartment series resistance errors. J Neurosci Methods 1998;86:25–34.